

## Excitons in T-shaped quantum wires

S. Glutsch and F. Bechstedt

*Friedrich-Schiller-Universität Jena, Institut für Festkörpertheorie und Theoretische Optik, Max-Wien-Platz 1, 07743 Jena, Germany*

W. Wegscheider and G. Schedelbeck

*Technische Universität München, Walter-Schottky-Institut, Am Coulombwall, 85748 Garching, Germany*

(Received 31 January 1997)

Binding energies and wave functions are calculated for the ground-state exciton in T-shaped quantum wires. It is shown that, if Coulomb interaction is taken into account, the hole is strongly localized by correlation with the electron. We demonstrate that no one-dimensional hole confinement is necessary for the formation of a one-dimensional exciton and that the exciton is roughly described by a two-dimensional hole, bound to a one-dimensional electron. Reasons are given for the shortcoming of the product Ansatz and the subband expansion for the pair wave function. For symmetric T structures with a thickness in the range from 5.4 to 7.0 nm, the calculated binding energies are larger than the values from approximate treatments, but smaller than the experimental results. [S0163-1829(97)04331-2]

### I. INTRODUCTION

More than a decade ago a new semiconductor structure was proposed, based upon a cleaved-edge overgrown superlattice.<sup>1,2</sup> The authors predicted that one-dimensional quantization is possible even without rigorous confinement in any of the space directions. Very recently, it was demonstrated theoretically that even quantum dots, i.e., zero-dimensional semiconductors, can be realized by twofold cleaved-edge overgrowth.<sup>3</sup>

In contrast to quantum-well wires, where the active region is completely surrounded by the barrier material, the origin of the one-dimensional bound states in T-shaped quantum wires is the expansion of the wave function into the larger available volume at the T-shaped junction of two quantum wells. Consequently, the exciton binding energy in such a T-shaped structure should be less than that in "conventional" quantum wires with comparable dimensions. Nevertheless, these structures are the subject of current intensive research and have been realized by several groups.<sup>4-11</sup> The reason for this is the fabrication technique. Lateral definition of quantum-well wires especially by etching techniques does not lead to sufficiently narrow wires with smooth interfaces. As a consequence, the binding energy of quantum-well wires hardly exceeds the value of the underlying quantum well, and the optical spectra reveal a large inhomogeneous broadening. In contrast, T-shaped quantum wires can be produced in a controlled way by molecular-beam epitaxy, with a quality, comparable to that of quantum wells. They are characterized by sizes less than the Bohr radius of the exciton and small thickness fluctuations.

While quantum-well wires are well understood,<sup>12</sup> the theory of T-shaped quantum wires is not developed to the same extent. In particular, the reasons for the extreme enhancement of the binding energy seen experimentally needs to be clarified. The numerical treatment is much more complicated because of the continuum degrees of freedom in all three space directions. Only the single-particle problem has been solved accurately.<sup>5,11,13-15</sup> Hitherto, the exciton prob-

lem was solved only by factorization or variational methods.<sup>13-15</sup> However, because of the strong delocalization of the hole, such approximations cannot give accurate results. Löffler *et al.* suggest a calculation that starts with a localized electron and then calculates the eigenstates of the hole in the Coulomb potential of the electron and the outer confinement. An interesting aspect is, whether one- or two-dimensional hole confinement is necessary for the formation of a one-dimensional exciton.

Experimentally, it is impossible to directly measure the binding energy by photoluminescence. Instead, the published numbers are determined from various experimental and theoretical data, with errors likely to accumulate. Therefore, it is important to have some theoretical predictions about what order of magnitude can be expected for the binding energy.

In this paper we numerically solve the two-particle problem within the effective-mass approximation. Scattering states of the electron and hole are fully taken into account. The resulting binding energy and oscillator strength is compared with results of a variational calculation. To study the nature of the hole confinement, we consider model cases where the hole confinement is only two dimensional or is totally neglected. Finally, single-particle and binding energies of different T-shaped wires are compared. The paper is organized as follows: in Sec. II, we introduce the basic equations; the numerical method is outlined in Sec. III; the results are presented in Sec. IV; and conclusions are drawn in Sec. V.

### II. BASIC EQUATIONS

We consider a sample that is based upon a GaAs-Ga<sub>1-x</sub>Al<sub>x</sub>As single quantum well, grown in [001] direction. After cleavage, successive layers of GaAs and Ga<sub>1-x</sub>Al<sub>x</sub>As are deposited onto the (110) surface. We identify the crystal orientations [110], [001], and [ $\bar{1}\bar{1}$ 0] with the  $x$ ,  $y$ , and  $z$  axes. The thicknesses of the (110) and (001) quantum wells are denoted as  $D_x$  and  $D_y$ , respectively. A sketch of the sample is shown in Fig. 1.

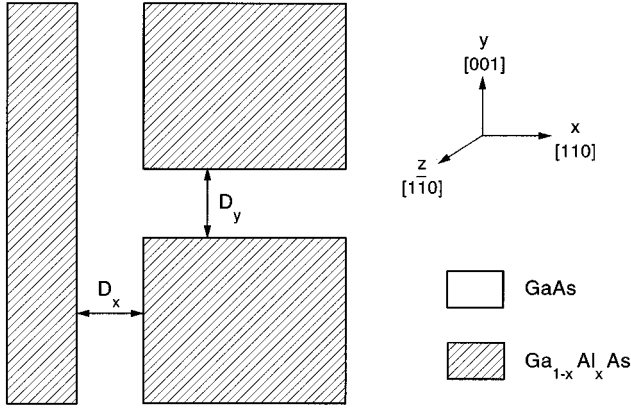


FIG. 1. Sketch of the T-shaped quantum wire under consideration, and notations.

Our theoretical description is based upon the two-band model in the effective-mass approximation with anisotropic hole mass. We use  $m_e = 0.0665m_0$  for the electron mass ( $m_0 = 9.109 \times 10^{-31}$  kg — electron rest mass) and a set of Luttinger parameters  $\gamma_1 = 6.85$ ,  $\gamma_2 = 2.10$ , and  $\gamma_3 = 2.90$ .<sup>16</sup> The hole masses are  $m_{hx} = m_{zh} = m_{hh[110]} = 2/(2\gamma_1 - \gamma_2 - 3\gamma_3)m_0 = 0.69m_0$  and  $m_{hy} = m_{hh[001]} = 1/(\gamma_1 - 2\gamma_2)m_0 = 0.38m_0$ . The spherically averaged heavy-hole mass is  $m_{hhs} = 1/(\gamma_1 - 0.8\gamma_2 + 1.2\gamma_3)m_0 = 0.59m_0$ , leading to a reduced heavy-hole exciton mass  $m = m_e m_{hhs}/(m_e + m_{hhs}) = 0.0598m_0$ . We assume a static dielectric constant  $\epsilon = 13.2$  and band offsets of the form  $H_e = \Delta E_c = 790x$  meV and  $H_h = \Delta E_v = 460x$  meV, with  $x$  being the aluminum mole fraction in the mixed crystal layer.<sup>17</sup> The vacuum dielectric constant is  $\epsilon_0 = 8.854 \times 10^{-12}$  As/(Vm). For this choice of parameters, the binding energy of the three-dimensional heavy-hole exciton is  $E_B = 1/2 m e^4 / [(4\pi\epsilon_0\epsilon)^2 \hbar^2] = 4.67$  meV and its Bohr radius is  $a_B = 4\pi\epsilon_0\epsilon \hbar^2 / (m e^2) = 11.6$  nm. The parameters are very close to those used by Someya *et al.*<sup>6,7</sup> and Gislason *et al.*<sup>9</sup>

First, we treat the quantum wells in the  $x$  and  $y$  directions separately, thus neglecting the coupling on the T intersection. The eigenfunctions in the growth direction and the corresponding energies obey one-dimensional stationary Schrödinger (Heisenberg) equations ( $p = e, h$ ;  $\xi = x, y$ ;  $m_{e\xi} = m_e$ ),

$$\left[ -\frac{\hbar^2}{2m_{p\xi}} \frac{d^2}{d\xi^2} + W_{p\xi}(\xi) \right] \varphi_{p\xi}(\xi) = E_{p\xi\lambda} \varphi_{p\xi\lambda}(\xi), \quad (1)$$

where

$$W_{p\xi}(\xi) = \begin{cases} 0 & \text{for } |\xi| < D_\xi/2 \\ H_p & \text{elsewhere.} \end{cases}$$

The discrete eigenvalues follow from the transcendental equations<sup>18</sup>

$$E_{p\xi} = \frac{\hbar^2 \pi^2}{2m_{p\xi} D_\xi^2} \beta_{p\xi}^2; \quad \left\{ \begin{array}{l} \cos\left(\frac{\pi}{2} \beta_{p\xi}\right) \\ \sin\left(\frac{\pi}{2} \beta_{p\xi}\right) \end{array} \right\} = C_{p\xi} \beta_{p\xi};$$

$$\beta > 0; \quad C_{p\xi}^2 = \frac{\hbar^2 \pi^2 / (2m_{p\xi} D_\xi^2)}{H_p}. \quad (2)$$

The discrete eigenvalues are labeled in ascending order with  $\lambda = 1, 2, \dots$  and a suppressed quantum number indicates the ground state ( $\lambda = 1$ ).

Now, we take into account the coupling of the quantum wells via the T intersection. In this case, the electron and hole motions satisfy

$$\left[ -\frac{\hbar^2}{2m_{px}} \frac{\partial^2}{\partial x^2} - \frac{\hbar^2}{2m_{py}} \frac{\partial^2}{\partial y^2} + T_p(x, y) \right] \varphi_{p\mu}(x, y) = E_{p\mu} \varphi_{p\mu}(x, y), \quad (3)$$

with

$$T_p(x, y) = \begin{cases} W_{px}(x) & \text{for } x < D_x/2 \\ W_{py}(y) & \text{for } x \geq D_y/2. \end{cases}$$

One-dimensional confinement is realized if the ground states of the T intersection  $E_p$  is below the lowest quantum-well ground states,  $\min(E_{px}, E_{py})$ . We call the differences

$$E_{cp} = \min(E_{px}, E_{py}) - E_p$$

electron and hole confinement energies. The sum

$$E_c = E_{ce} + E_{ch}$$

is referred to as the wire confinement energy, or simply, confinement energy. It is a common belief<sup>7,11,14</sup> that the largest exciton binding energy is obtained when  $E_c$  reaches its maximum. In the case of one-dimensional confinement, the wave functions  $\varphi_p$  can be normalized to unity, and  $|\varphi_p(x, y)|^2$  is interpreted as the probability density of the particle  $p$ .

In the next step, we take into account Coulomb interaction between electron and hole. After separation of center-of-mass and relative motion in the  $z$  direction we end up with the exciton equation,

$$(\hat{H}\varphi_\nu)(x_e, y_e, x_h, y_h, z) = E_\nu \varphi_\nu(x_e, y_e, x_h, y_h, z), \quad (4)$$

where

$$\hat{H} = \sum_{p \in \{e, h\}} \left[ -\frac{\hbar^2}{2m_{px}} \frac{\partial^2}{\partial x_p^2} - \frac{\hbar^2}{2m_{py}} \frac{\partial^2}{\partial y_p^2} + T_p(x_p, y_p) \right] - \frac{\hbar^2}{2m_z} \frac{\partial^2}{\partial z^2} + V(x_e - x_h, y_e - y_h, z),$$

$$\frac{1}{m_z} = \frac{1}{m_{ze}} + \frac{1}{m_{zh}}; \quad V(x, y, z) = -\frac{e^2}{4\pi\epsilon_0\epsilon \sqrt{x^2 + y^2 + z^2}}.$$

The binding energy of the one-dimensional exciton is defined as the ground-state energy of the interaction-free electron-hole pair minus the ground-state energy of the two-particle equation,

$$E_b = E_e + E_h - E.$$

The oscillator strength per unit length  $|f|^2$  is the modulus square of the integrated wave function, taken at equal electron and hole positions:

$$|f|^2 = \left| \iint dX dY \varphi(X, Y, X, Y, 0) \right|^2.$$

Intuitively it is plausible that  $|f|^2$  increases with the localization of wave functions. This has also been confirmed by experiments.<sup>8</sup> The functions

$$|\tilde{\varphi}_p(x, y)|^2 = \iiint dx_{\bar{p}} dy_{\bar{p}} dz |\varphi(x_e, x_h, y_e, y_h, z)|^2 \quad (\bar{e} = h, \bar{h} = e)$$

represent conditional probability densities and play the role of the functions  $|\varphi_p|^2$  in the interaction-free case. Furthermore, we define a correlation function

$$|\tilde{\varphi}_p(z)|^2 = \iiint dx_e dy_e dx_h dy_h |\varphi(x_e, x_h, y_e, y_h, z)|^2,$$

which can be interpreted as the probability density of the one-dimensional exciton.

An approximate solution of Eq. (4) for the lowest subband has been proposed by Chang *et al.*<sup>2</sup> in the form

$$\varphi_\lambda(x_e, y_e, x_h, y_h, z) = \varphi_e(x_e, y_e) \varphi_h(x_h, y_h) \varphi_{z\lambda}(z), \quad (5)$$

with a variational function  $\varphi_{z\lambda}$ . By inserting the ansatz (5) in Eq. (4), an effective one-dimensional equation for the motion in the wire direction is obtained:

$$\left[ E_e + E_h - \frac{\hbar^2}{2m_z} \frac{d^2}{dz^2} + V_{\text{eff}}(z) \right] \varphi_{z\lambda}(z) = E_\lambda \varphi_{z\lambda}(z), \quad (6)$$

where

$$V_{\text{eff}}(z) = \iiint dx_e dy_e dx_h dy_h |\varphi_e(x_e, y_e)|^2 \times |\varphi_h(x_h, y_h)|^2 V(x_e - x_h, y_e - y_h, z).$$

Equation (6) has only qualitative character for two reasons: (i) the convergence of the one-subband approximation is very slow in one-dimensional structures,<sup>19</sup> and (ii) the assumption  $|\varphi_p|^2 \approx |\tilde{\varphi}_p|^2$  on which the factorization (5) is based is strongly violated for the hole, as we will demonstrate in Sec. IV.

### III. NUMERICAL PROCEDURE

In this section we specify how the ground state is calculated numerically. The solutions of Eq. (2) can be found using a pocket calculator. Equation (3) can be solved by standard techniques.<sup>14,15</sup> An application of those methods to the two-particle problem is not feasible because it would

exceed the resources of memory and computing time. Hitherto, Eq. (4) has been treated approximately by variational methods,<sup>2,15,14</sup> but a complete numerical solution has not been accomplished so far. Therefore, we shall concentrate mainly on how to solve Eq. (4). For all explicit calculations we use dimensionless quantities, defined by the convention  $\hbar = e^2/(4\pi\epsilon_0\epsilon) = m = 1$ . Energies and lengths are then measured in units of  $2E_B$  and  $a_B$ , respectively.

The Hamiltonian in Eq. (4) can be written in the form:

$$\hat{H} = \sum_{\alpha=1}^m \left( -\frac{1}{2m_\alpha} \frac{\partial^2}{\partial \xi_\alpha^2} \right) + U(\vec{\xi}). \quad (7)$$

Introducing a uniform grid  $G = \{\vec{\xi}_i\}_{i=1}^N$  with mesh sizes  $\Delta \vec{\xi} = (\Delta \xi_1, \dots, \Delta \xi_m)$ , a function  $\psi$  is represented by an  $N$ -dimensional vector  $\vec{\psi} = (\psi_1, \dots, \psi_N)$ , where  $\psi_i = \psi(\vec{\xi}_i)$ . A discretization of the operator (7) can be performed by

$$\left( \frac{\partial^2}{\partial \xi_\alpha^2} \psi \right)_i = \frac{\psi(\vec{\xi} - \Delta \xi_\alpha \vec{e}_\alpha) - 2\psi(\vec{\xi}) + \psi(\vec{\xi} + \Delta \xi_\alpha \vec{e}_\alpha)}{(\Delta \xi_\alpha)^2},$$

$$(U\psi)_i = U_i \psi(\vec{\xi}_i).$$

The single-particle potentials are discretized according to  $T_{pj} = T_p(\vec{\xi}_j)$  and the Coulomb potential  $V$  is replaced by<sup>20</sup>

$$V_j = \frac{\frac{1}{2} (\Delta \varphi_{\text{g.s.}})_j}{\varphi_j} + E_{\text{g.s.}},$$

where  $E_{\text{g.s.}} = -\frac{1}{2}$  and  $\varphi_{\text{g.s.}}(x, y, z) = \exp(-\sqrt{x^2 + y^2 + z^2})$  are the ground-state energy and wave function of the three-dimensional hydrogen problem. The matrix  $H$ , resulting from the discretization of the Hamiltonian  $\hat{H}$  [Eq. (7)], is sparse, i.e., only  $O(N)$  of its elements are nonzero. Furthermore,  $H$  is Hermitian and has real eigenvalues  $E_1, \dots, E_N = E_{\text{max}}$  and orthonormal eigenvectors  $\vec{\varphi}_1, \dots, \vec{\varphi}_N$ . As the mesh sizes are reduced, the largest eigenvalue is mainly determined by the operator of the kinetic energy, and it holds that

$$E_{\text{max}} \leq \sum_{\alpha=1}^m \frac{2}{m_\alpha (\Delta \xi_\alpha)^2} + \max\{U_j\}.$$

In order to find the ground-state vector  $\vec{\varphi}$  of the matrix  $H$ , we consider a sequence  $\{\vec{\varphi}^{(k)}\}_{k=0}^\infty$  defined by a recurrence relation

$$\vec{\varphi}^{(k+1)} = \frac{\vec{\varphi}^{(k)} - qH\vec{\varphi}^{(k)}}{\|\vec{\varphi}^{(k)} - qH\vec{\varphi}^{(k)}\|}.$$

Provided that  $(\vec{\varphi}, \vec{\varphi}^{(0)}) \neq 0$ , it holds that  $\lim_{k \rightarrow \infty} \vec{\varphi}^{(k)} = \vec{\varphi}$  if  $0 < q < 2/(E_{\text{max}} + E_1)$ . The number of iterations is determined by the slow decrease of the lowest-order excited states, and is in the order of  $E_{\text{max}}/(E_2 - E_1)$ . However, the convergence can be considerably accelerated by using a basic idea of the multigrid method.<sup>21</sup> We assume that  $\vec{\varphi}[G_l]$  is the ground state of  $\hat{H}$ , discretized on a grid  $G_l$ . To find the ground state  $\vec{\varphi}[G_{l+1}]$  on a refined grid  $G_{l+1} \supset G_l$ , we start

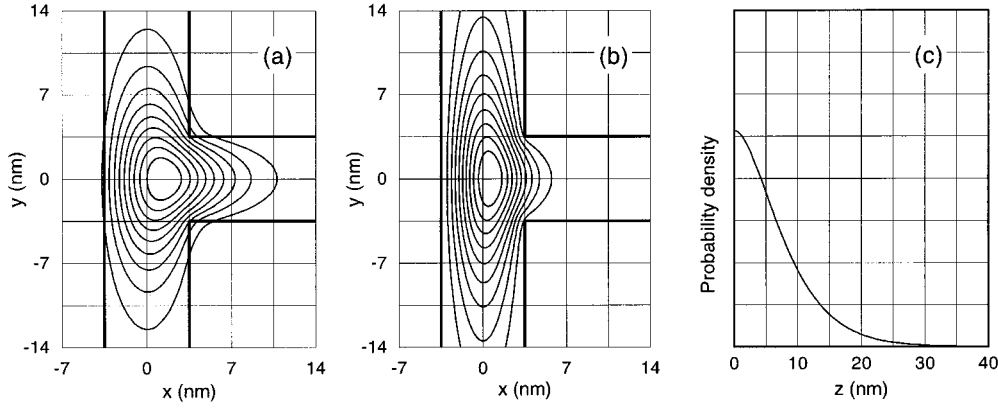


FIG. 2. One-particle properties: (a) probability density of the electron,  $|\varphi_e|^2$ ; (b) probability density of the hole,  $|\varphi_h|^2$ ; and (c) ground-state probability density  $|\varphi_z|^2$  obtained from the effective one-dimensional problem.

the iteration with initial values  $\vec{\varphi}^{(0)}[G_{l+1}]$ , determined by interpolation between the values of  $\vec{\varphi}[G_l]$ . The error  $\vec{\varphi}^{(0)}[G_{l+1}] - \vec{\varphi}[G_{l+1}]$  is dominated by large-wave vector, high-energy components that are efficiently suppressed by a relaxation parameter  $q = 1/E_{\max}[G_{l+1}]$ , while the small-wave vector, low-energy components are vanishingly small. Starting from some coarse grid  $G_0$ , the solution is calculated by successive refinement  $G_0 \subset \dots \subset G_n = G$ , where the iteration on each grid is terminated when machine accuracy is reached.

Another important issue is the accuracy, since the mesh sizes cannot be made arbitrarily small for the solution of the full two-particle problem (4). A binding energy calculated from the exact single-particle energies,  $E_p$ , and the numerical value of  $E$  according to  $E_b = E_e + E_h - E[G]$  is subject to the full discretization error of  $E[G]$ . A partial compensation of the discretization errors can be achieved when the single-particle energies are calculated with the same finite mesh sizes:  $E_b = E_e[G] + E_h[G] - E[G]$ . This is equivalent to replacing to discretizing the single-particle potentials according to  $T_{pj} = T_p(\vec{\xi}_j) + E_p - E_p[G]$ , so that the exact value of  $E$  is recovered for  $V=0$ . But one can go even further and assure that both  $E$  and  $\varphi(\vec{\xi}_j)$  coincide with the exact solutions for  $V=0$  by using potentials of the form

$$T_{pj} = \frac{\left[ \left( \frac{1}{2m_{px}} \frac{\partial^2}{\partial x^2} + \frac{1}{2m_{py}} \frac{\partial}{\partial y^2} \right) \varphi_p \right]_j}{\varphi_{p1j}} + E_p.$$

The above discretization was found to give an error that is about 3 times smaller than for the partial compensation, and about 30 times smaller than for the crude method.

#### IV. RESULTS

In this section we present numerical solutions of the equations in Sec. II. We consider the following samples: sample  $W$  with well thicknesses  $D_x = D_y = D = 7$  nm and an aluminum content of  $x = 0.35$ , studied by Wegscheider *et al.*;<sup>5</sup> and samples  $S_1$  with  $D = 5.4$  nm,  $x = 0.30$  and  $S_2$  with  $D = 5.3$  nm and AlAs barriers ( $x = 1$ ), studied by Someya *et al.*<sup>7</sup> The single-particle properties (3), the excitonic ground state (4), the result of the variational treatment (5), and the

influence of the hole confinement are discussed in detail for the sample  $W$ . Then, in order to study the dependence on the well thickness and the barrier heights, we compare the data of the samples  $W$ ,  $S_1$ , and  $S_2$ .

The single-particle energies for the sample  $W$  were found to be  $E_{ex} = E_{ey} = 56.2$  meV,  $E_{hx} = 8.0$  meV,  $E_{hy} = 13.2$  meV,  $E_e = 47.2$  meV,  $E_h = 7.5$  meV,  $E_{ce} = 9.0$  meV,  $E_{ch} = 0.5$  meV, and  $E_c = 9.5$  meV. Obviously, the one-dimensional confinement for the hole is much smaller than that for the electron. The theoretical results are very close or identical to those of Wegscheider *et al.* with  $E_c = 10$  meV, Kiselev and Rössler with  $E_{ce} = 9.0$  meV, and Bryant *et al.* with  $E_c = 9.6$  meV.

The single-particle densities  $|\varphi_p|^2$  and the modulus square of the correlation function  $|\varphi_z|^2$  are shown in Figs. 2(a) and (b). The contours represent lines of constant probability  $|\varphi_p(x,y)|^2 / \max|\varphi_p(x,y)|^2 = 0.1, 0.2, \dots, 0.9$ . Obviously, the localization of the electron is much stronger than that of the hole. The reason is not the difference in the dimensionless parameters (2),  $C_{ex} = 0.64$  versus  $C_{hx} = 0.26$ , but the anisotropic hole mass; since  $E_{hy} > E_{hx}$ , a penetration of the hole into the (001) quantum well is not energetically favorable.

Since our analysis is limited to heavy holes only, an important question is whether this picture is changed when valence-band mixing is taken into account. This point was addressed in previous publications.<sup>11,13</sup> The results of both papers for the heavy hole are in qualitative agreement with those of the present paper. At the same time, there is some controversy about the localization of the light hole. Langbein *et al.*<sup>11</sup> found that the light hole behaves similar as the heavy hole, whereas Löffler and co-workers<sup>13</sup> predict a stronger localization for the light hole.

The product ansatz (5) yields a binding energy of 10.1 meV. The modulus square of the wavefunction,  $|\varphi_z|^2$ , is shown in Fig. 2(c). In contrast to three- or two-dimensional excitons, the wave function of the effective one-dimensional exciton does not have a kink for  $z = 0$ , because the effective one-dimensional Coulomb potential is finite for  $z = 0$ .

The two-particle problem (4) was solved using mesh sizes  $\Delta x_e = \Delta y_e = \Delta x_h = \Delta y_h = \frac{1}{8}D$  and  $\Delta z = \frac{5}{8}D$ . The result for the binding energy is  $E_b = (13.2 \pm 0.2)$  meV. The experimental value is 17 meV (Ref. 5) and Bryant *et al.* obtained 9.6 meV, although their value for  $E_c$  is somewhat larger than ours.

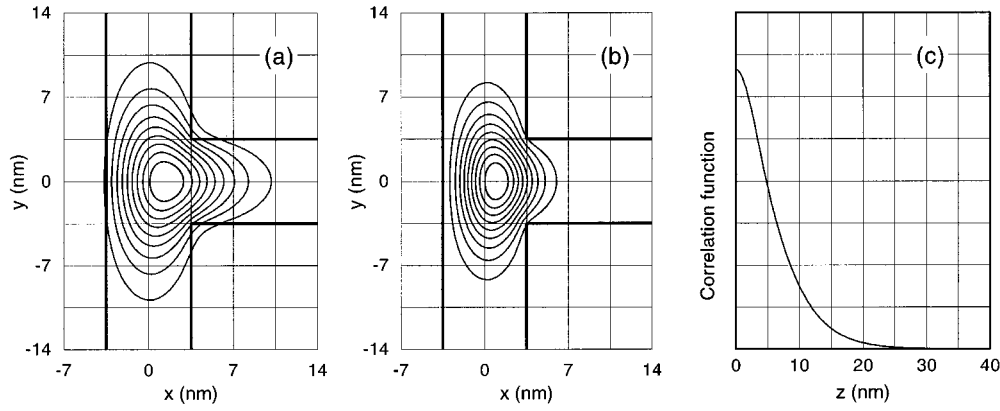


FIG. 3. Two-particle properties: (a) conditional probability density of the electron,  $|\tilde{\varphi}_e|^2$ ; (b) conditional probability density of the hole,  $|\tilde{\varphi}_h|^2$ ; and correlation function  $|\tilde{\varphi}_z|^2$  for the  $z$  direction.

The conditional probability densities  $|\tilde{\varphi}_p|^2$  are shown in Figs. 3(a) and (b). Surprisingly, the hole is much more localized than the electron, in contrast to the situation for interaction-free particles. A simplified explanation can be given by decoupling the center-of-mass and relative motion such that  $\varphi(x_e, y_e, x_h, y_h, z) = \varphi_{\text{c.m.}}(X, Y) \varphi_{\text{rel}}(x, y, z)$  with center-of-mass and relative coordinates defined in the usual way:

$$\Xi = \frac{m_e \xi_e + m_h \xi_h}{m_e \xi_e + m_h \xi_h}; \quad \xi = \xi_e - \xi_h; \quad (\Xi = X, Y; \quad \xi = x, y).$$

As a measure for the extension of the wave functions, we use the mean variances, generally defined as  $\sigma^2(A) = \langle \hat{A}^2 \rangle - \langle \hat{A} \rangle^2$ . One easily verifies that

$$\sigma^2(\xi_e) = \sigma^2(\Xi) + \left( \frac{m_h \xi_h}{m_e \xi_e + m_h \xi_h} \right)^2 \sigma^2(\xi),$$

$$\sigma^2(\xi_h) = \sigma^2(\Xi) + \left( \frac{m_e \xi_e}{m_e \xi_e + m_h \xi_h} \right)^2 \sigma^2(\xi).$$

Since the electron mass is much smaller than the hole masses, the extension of the hole wave function is smaller than the extension of the electron wave function.

The correlation function  $|\tilde{\varphi}_z|^2$  is shown in Fig. 3(c). There is no essential difference to  $|\varphi_z|^2$  [cf. Fig. 2(c)], except that the localization of  $|\tilde{\varphi}_z|^2$  is stronger, which becomes clear from the higher binding energy.

Bryant *et al.* point out that intercoupling of wires becomes important when the structure is based upon a superlattice.<sup>22</sup> As follows from Figs. 2 and 3, this is not the case for the uncorrelated electron and the exciton when the interlayer spacing is larger than 20 nm, such as in Refs. 5,6,8,10. A significant influence from the hole is not expected, because (i) the energy  $E_{hy}$  is also lowered due to interwell coupling, thus partially compensating the reduction of  $E_h$ , and (ii) the contribution of the hole to the confinement energy  $E_c$  is much smaller than the contribution of the electron anyway.

From the previous calculation we learned that (i) the one-dimensional confinement is dominated by the electron and that (ii) the localization of the hole is mainly due to the

Coulomb attraction to the localized electron. This raises the question of whether one-dimensional hole confinement is necessary for the formation of a quantum-wire exciton. For a quantitative study, we consider two model cases,  $M_1$  and  $M_2$ . For  $M_1$  we only allow for a two-dimensional hole confinement in the (110) quantum well, i.e.,  $T_h(x, y) = W_h(x)$ ; and no confinement, i.e.,  $T_h(x, y) = 0$ , is assumed for  $M_2$ . A one-dimensional excitonic bound state is observed in both cases with a binding energy of  $E_b = 12.0$  meV for  $M_1$  and  $E_b = 9.8$  meV for  $M_2$ . Furthermore, despite the lack of one-dimensional confinement, the localization of the hole was stronger than the localization of the electron in both cases. This model calculation also shows that the binding energy for  $M_1$  is closer to the binding energy of the sample  $W$  than to the result of the variational calculation. Even though we have found that a one-dimensional hole bound state truly exists, the latter findings show that an exciton in a T-shaped quantum wire is nearly built up by a two-dimensional hole, bound to a one-dimensional electron.

In the light of these results, it is worthwhile to discuss the quality of the approximation (5). The variational treatment considerably underestimates the binding energy. The reason is the strong deviation of  $|\tilde{\varphi}_h|^2$  from  $|\varphi_h|^2$ . The variational result is even smaller than the binding energy of example  $M_1$ , where the hole is completely delocalized. Since the true excitonic binding energy is rather insensitive to the single-particle hole wave function, the approximation (5) is ambiguous and should not even give the right trends if the structure is to be optimized. The variational result for the oscillator strength  $|f|^2$  is disastrous:  $0.047 \text{ nm}^{-1}$  versus  $0.145 \text{ nm}^{-1}$  for the full solution.

It is important to note that no significant increase of accuracy is expected, when Eq. (6) is extended to all one-dimensional subbands. The reason for this is that the subband energies become continuous if the energy exceeds  $E_{ch}$ , which is very small compared with the binding energy. In most cases of practical interest, there is only one hole bound state, and it holds that  $|\tilde{\varphi}_h|^2 = |\varphi_h|^2$ , which was found to be the main reason for the failure of the variational method.

Nevertheless, since the solution of Eq. (4) requires extensive computations, it is desirable to have a simple method that yields a reasonable estimate for  $E_b$ . For example, if

TABLE I. Comparison of different samples (models). All units are in meV.

Sample (model)	W	$M_1$	$M_2$	$S_1$	$S_2$
$E_e$	56.2	56.2	56.2	63.4	93.5
$E_h$	7.5	8.0	0.0	11.2	13.9
$E_{ce}$	9.0	9.0	9.0	10.7	19.2
$E_{ch}$	0.5	0.0	0.0	0.9	1.1
$E_c$	9.5	9.0	9.0	11.6	20.3
$E_b$	13.2	12.0	9.8	14.3	16.4
$E_b$ , exp.	17 <sup>a</sup>			17 <sup>b</sup>	27 <sup>b</sup>

<sup>a</sup>From Ref. 5.

<sup>b</sup>From Ref. 7.

$\varphi_e$  and  $\varphi_h$  are also variational functions, then the accuracy is increased—even  $M_1$  and  $M_2$  could be treated in this way—, while the complexity is not fundamentally changed; instead of Eqs. (3) and (6), a set of three coupled Heisenberg equations has to be solved self-consistently. Grundmann and Bimberg<sup>3</sup> proposed an ansatz of the form  $\Psi_{\text{ex}}(\mathbf{r}_e, \mathbf{r}_h) = \Psi_e(\mathbf{r}_e)\Psi_h(\mathbf{r}_h)$  for the exciton wave function  $\Psi_{\text{ex}}$  that depends on six space coordinates. The resulting two coupled Heisenberg equations show a fast convergence, and the accuracy is significantly improved, compared to Eq. (5).

To study the influence of the well thicknesses and the barrier heights, we have repeated the calculation for the samples  $S_1$  and  $S_2$ . For the electron confinement in sample  $S_2$ , we use the energy difference of the direct transitions,  $H_e = \Delta E_c(\Gamma_6) = 790$  meV. This is certainly the better approximation when phonon-assisted transitions are unimportant, but has a tendency to overestimate the binding energy. The results are summarized in Table I. For completeness, we also incorporate the models  $M_1$  and  $M_2$ .

As expected, the binding energy increases for smaller well thicknesses or larger aluminum contents. For the electron, the effect of the aluminum concentration on the confinement energy is much stronger than the effect of the well thickness. The exact opposite is the case for the hole, because the hole already “sees” infinite barriers for  $x=0.30$ . It is also found true for T-shaped quantum wires that  $E_b$  increases as  $E_c$  increases. However, the relative increase of  $E_b$  is smaller than the relative increase of  $E_c$ . This relationship is also not universal, as becomes clear from the comparison of  $M_1$  and  $M_2$ , which both have a wire confinement energy of 9.0 meV, but quite different binding energies. Therefore, a structure optimization based on single-particle confinement energy<sup>11,14</sup> can only serve as guideline. A definite answer can only be given by a solution of the two-particle problem for a large variety of well thicknesses and aluminum contents.<sup>23</sup>

In all cases, the theoretical result for  $E_b$  was found to be smaller than the experimental result. Therefore, we shortly discuss the influences of the approximations made in our theoretical model. It is known that nonparabolicity and dielectric mismatch lead to an increase of the binding energy for small quantum-well thicknesses.<sup>24</sup> On the other hand, it was claimed that the wire binding energy is rather insensitive to the electron mass.<sup>15</sup> To see the order of magnitude, we repeated the calculations with the thickness-dependent electron masses given by Andreani and Pasquarello,<sup>24</sup> namely,  $m_e = 0.074, 0.076,$  and  $0.084m_0$  for  $W, S_1,$  and  $S_2$ . The resulting binding energies are 13.9, 15.3, and 17.9 meV. There is indeed an increase in the binding energy, but the enhancement is less than for quantum wells. Taking into account the dielectric mismatch, the measured values for  $W$  and  $S_1$  can be explained by theory. Another effect has not yet been taken into account, namely, that the exciton binding energy is of the same order of magnitude as the energy of the optical phonon. Consequently, the effective static dielectric constant is in between the static value  $\epsilon_s$  and the high-frequency limit  $\epsilon_\infty$  and leads to an increase of  $E_b$ . This influence becomes larger as the binding energy increases.

## V. SUMMARY

We have performed an accurate numerical calculation of the ground-state exciton in a T-shaped quantum-well wire, in the effective-mass approximation. We have found that the Coulomb-correlated hole is strongly localized, in contrast to the interaction-free case. This was identified as the main reason for the failure of the variational calculation. It was demonstrated that one-dimensional hole confinement is not necessary for the formation of a one-dimensional exciton and that a two-dimensional hole, bound to a one-dimensional electron, is a good approximation for an exciton in a T structure. For the samples  $W$  and  $S_1$ , the calculated binding energies are found to be slightly smaller than the experimental results, but the difference can be explained by taking into account the assumptions that have been made in our simplified model. For  $S_2$  our results seem to be in contradiction to the experiment.

## ACKNOWLEDGMENTS

The authors are indebted to J.M. Baker, G.W. Bryant, M. Grundmann, J.M. Hvam, and W. Langbein for interesting discussions or communicating results prior to publication. Two of the authors (W.W. and G.S.) also acknowledge financial support from the Deutsche Forschungsgemeinschaft in the framework of Sonderforschungsbereich 348.

<sup>1</sup>H.L. Störmer (unpublished).

<sup>2</sup>Y.C. Chang, L.L. Chang, and L. Esaki, Appl. Phys. Lett. **47**, 1324 (1985).

<sup>3</sup>M. Grundmann and D. Bimberg, Phys. Rev. B **55**, 4054 (1997).

<sup>4</sup>A.R. Goñi, L.N. Pfeiffer, K.W. West, A. Pinczuk, H.U. Baranger,

and H.L. Störmer, Appl. Phys. Lett. **61**, 1956 (1992).

<sup>5</sup>W. Wegscheider, L.N. Pfeiffer, M.M. Dignam, A. Pinczuk, K.W. West, S.L. McCall, and R. Hull, Phys. Rev. Lett. **71**, 4071 (1993).

<sup>6</sup>T. Someya, H. Akiyama, and H. Sakaki, Phys. Rev. Lett. **74**, 3664 (1995).

- <sup>7</sup>T. Someya, H. Akiyama, and H. Sakaki, *Phys. Rev. Lett.* **76**, 2965 (1996).
- <sup>8</sup>H. Akiyama, T. Someya, and H. Sakaki, *Phys. Rev. B* **53**, R16 160 (1996).
- <sup>9</sup>H. Gislason, C.B. Sørensen, and J.M. Hvam, *Appl. Phys. Lett.* **69**, 800 (1996).
- <sup>10</sup>H. Gislason, W. Langbein, and J.M. Hvam, *Appl. Phys. Lett.* **69**, 3248 (1996).
- <sup>11</sup>W. Langbein, H. Gislason, and J.M. Hvam, *Phys. Rev. B* **54**, 14 595 (1996); H. Gislason, W. Langbein, and J.M. Hvam, *Superlattices Microstruct.* (to be published).
- <sup>12</sup>For most recent results, see A.N. Forshaw and D.M. Whittaker, *Phys. Rev. B* **54**, 8794 (1996).
- <sup>13</sup>A. Löffler, D. Brinkmann, and G. Fishman, in *Semiconductor Heteroepitaxy. Growth, Characterization and Device Applications*, edited by B. Gil and R.-L. Aulombard (World Scientific, Singapore, 1995), p. 375.
- <sup>14</sup>A.A. Kiselev and U. Rössler, *Semicond. Sci. Technol.* **11**, 203 (1996).
- <sup>15</sup>G.W. Bryant, P.S. Julienne, and Y.B. Band, *Superlattices Microstruct.* **20**, 601 (1996).
- <sup>16</sup>*Physics of Group IV Elements and III-V Compounds*, edited by O. Madelung, M. Schulz, and H. Weiss, Landoldt-Börnstein, New Series, Group III, Vol. 17, Pt. a (Springer, Berlin, 1982).
- <sup>17</sup>S. Adachi, *GaAs and Related Materials* (World Scientific, Singapore, 1994).
- <sup>18</sup>S. Flügge and H. Marschall, *Rechenmethoden der Quantentheorie*, Erster Teil (Springer-Verlag, Berlin, 1952).
- <sup>19</sup>S. Glutsch and D.S. Chemla, *Phys. Rev. B* **53**, 15 902 (1996).
- <sup>20</sup>S. Glutsch, D.S. Chemla, and F. Bechstedt, *Phys. Rev. B* **54**, 11 592 (1996).
- <sup>21</sup>W. Hackbusch, *Iterative Solution of Large Sparse Systems of Equations* (Springer, New York, 1994).
- <sup>22</sup>G.W. Bryant, P.S. Julienne, and Y.B. Band, *Surf. Sci.* **361/362**, 801 (1996).
- <sup>23</sup>S. Glutsch, F. Bechstedt, W. Wegscheider, and G. Schedelbeck (unpublished).
- <sup>24</sup>L.C. Andreani and A. Pasquarello, *Phys. Rev. B* **42**, 8928 (1990).